16TH EUROPEAN CONFERENCE ON EARTHQUAKE ENGINEERING THESSALONIKI 18 - 21 JUNE 2018

INFLUENCE OF MASONRY STEEL REINFORCEMENT ON THE IN-PLANE BEHAVIOR OF INFILLED RC FRAMES

Anastasios DROUGKAS[1], Chrissy-Elpida ADAMI[2], Elizabeth VINTZILEOU[3], Vasiliki PALIERAKI[4]

ABSTRACT

Numerous typologies for the layout of steel bars in reinforced masonry members have been proposed in the literature and in relevant design codes. Given that such reinforcement can increase the load-bearing capacity and ductility while also reducing the susceptibility to damage of clay block masonry members, it follows that it can also enhance the behavior of such members in their role as infill in reinforced concrete frames. This contribution may be crucial in the structural safety of new and existing reinforced concrete structures in seismic prone areas.

In this paper, the structural role of steel reinforcement bars embedded in the masonry infill of reinforced concrete frames is investigated. The infill masonry was designed around a clay block unit developed and granted a patent in the framework of the INSYSME project (http://www.insysme.eu/). Building upon the results of a rigorous experimental campaign, the function of the reinforcement bars is examined through numerical simulation of the response of concrete frames subjected to in-plane loading. The reinforcement bars are employed in different layouts within the body of the masonry. The infill is studied both individually, as a stand-alone structural element, as well as in models incorporating the infill, frame elements and the structural interaction of the two components.

The behavior of the studied layouts is compared in terms of structural stiffness, peak force, ductility and obtained damage pattern. Additionally, a comparison with experimental results is also presented. The results of this investigation contribute to the understanding of the structural function of reinforced masonry infills in concrete frames subjected to seismic loading.

Keywords: Reinforced masonry; clay block masonry; reinforced concrete; infilled frames; numerical analysis

1. INTRODUCTION

The behavior of brick masonry infills, widely used as enclosures to RC buildings, has been the subject of numerous experimental and analytical studies, during the last decades. Brick masonry infills offer an economic and durable solution, as they may ensure adequate insulation properties, whereas they may contribute to the seismic behavior of the structural system. It is noted that, enclosures and partition walls in RC structures are considered as non-structural elements and they are not explicitly taken into account in the aseismic design of new buildings. Nevertheless, theory and practice have repeatedly proven that

[1]Post-doctoral researcher, Faculty of Civil Engineering, National Technical University of Athens, Greece, adrougk@central.ntua.gr
[2]Post-doctoral researcher, Faculty of Civil Engineering, National Technical University of Athens, Greece, adamis@central.ntua.gr
[3]Professor, Faculty of Civil Engineering, National Technical University of Athens, Greece, elvintz@central.ntua.gr
[4]Post-doctoral researcher, Faculty of Civil Engineering, National Technical University of Athens, Greece, vasopal@central.ntua.gr

masonry infills may affect in a positive or negative way the seismic behavior of buildings, depending on their distribution along the plan and the height of the building and on the relative strength and stiffness of the infill walls and the surrounding frames. On the other hand, Eurocode 8 (CEN 2005) suggests that masonry infills should not be taken into account for the analysis of new RC buildings, whereas it includes some empirical measures for the limitation of damage on masonry infills caused by earthquakes, as well as (mainly) qualitative design rules for the RC frame-masonry infill interaction.

These open issues were the starting point for the EU-funded research project INSYSME (http://www.insysme.eu/). The project aims at developing innovative systems for masonry infills to be used for RC framed buildings, to derive concepts for their analysis and to develop simple and efficient methods for their design in everyday practice.

Within the framework of INSYSME, two innovative solutions for infill walls were developed by the authors and a Greek brick manufacturing industry XALKIS S.A. One of the proposed solutions, INSYSTEM 2, aims at enhancing the in-plane and out-of-plane deformability of the infill wall. A special, vertically perforated, brick unit has been designed and produced (Vintzileou et al. 2017). The innovative brick unit was granted a patent (No. 1008797) by the Greek Patent Office. Although the idea of reinforcing the infill wall is quite common, the use of the available in the market vertically perforated bricks allows for positioning of the horizontal reinforcement, whereas (as the infill is constructed after the completion of the RC structure) only external vertical reinforcement can be provided to the infill. The application of reinforced mortar plaster to the infills has been studied by several researchers (Calvi and Bolognini 2001; Ezzatfar et al. 2014; Facconi et al. 2012; Ghobarah and Mandooh Galal 2004; Leite and Lourenço 2012; Da Porto et al. 2013, 2015). The use of bed joint reinforcement has been studied and its positive effect on the behavior of masonry has been already proved, both in in-plane and out-of-plane loading (Masia, Simundic, and Page 2016; Penna, Calvi, and Bolognini 2007; Vermeltfoort 2016; Vintzileou and Palieraki 2007). The brick unit developed at the NTUA allows for efficient positioning of both horizontal and vertical reinforcement within the thickness of the infill, whereas it also allows for accommodation of electrical and plumbing installations in the vertical holes that are not reinforced.

In order to evaluate the performance of the system, in-plane and out-of-plane tests on one-bay infilled frames were performed. The numerical results of the analysis of the tested frames are validated with the experimental ones. In the present paper, the function of the reinforcement bars is examined through numerical simulation of the response of concrete frames subjected to in-plane loading. The reinforcement bars are employed in different layouts within the body of the masonry. The results of this investigation contribute to the understanding of the structural function of reinforced masonry infills in concrete frames subjected to seismic loading.

2. EXPERIMENTAL RESULTS

The masonry infill system tested is entitled INSYSTEM 2 and consists in a single leaf clay masonry infill (Fig. 1a). The enclosure is not fixed to the RC frame elements

INSYSTEM 2, in which the infill may be horizontally and/or vertically reinforced, depending on the percentage of the reinforcement that is used, may be applied in medium to high seismicity areas. To serve the purpose of the system, a special unit, 320mm in length, 235mm in height and 280mm in thickness, was designed by NTUA and XALKIS (Fig. 1b). The horizontal reinforcement is positioned in the bed joints during the construction of the wall, whereas the vertical reinforcement is placed in vertical holes after the construction of the wall. The enclosure is not fixed to the RC frame elements, as a mortar joint is provided along the surrounding infill-to-RC concrete interfaces. A detailed description of the brick unit is provided elsewhere (Vintzileou et al. 2017).

The behavior of the infill INSYSTEM 2 was investigated experimentally through in-plane cyclic and repeated out-of-plane tests. The dimensions of the infill were approximately equal to 3.00x2.30 [m^2]. The results of in-plane testing are briefly presented here.

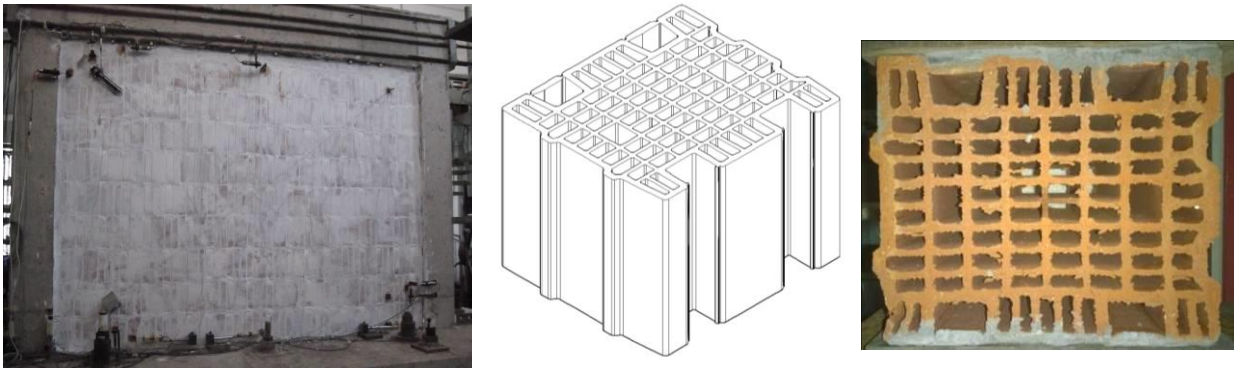

(a) (b)

Figure 1. (a) Infill wall constructed using the new brick (INSYSTEM 2) for in-plane loading, (b) Innovative Brick unit.

Horizontal cyclic displacements are imposed at mid-height of the top RC beam, using a hydraulic jack of ±1000kN maximum capacity. The specimen tested under in-plane actions is only horizontally reinforced (ρ=0.35%). The horizontal reinforcement, located at every other mortar bed joint, consists in prefabricated trusses (Murfor RND). The bed joint reinforcement consists of two parallel wires, 5mm diameter, welded together with a continuous truss wire of 3.75mm diameter. The distance between the two parallel wires is equal to 200mm.

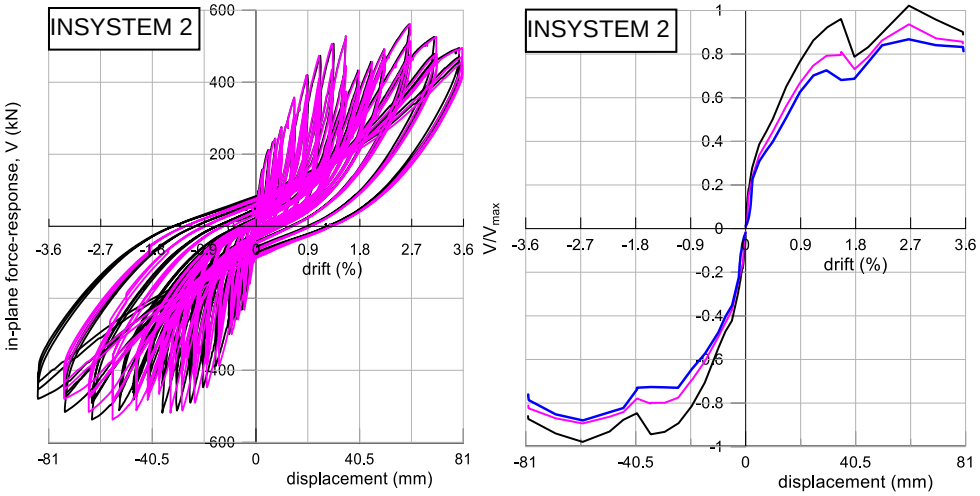

(a) (b)

Figure 2. In-plane test of INSYSTEM 2. (a) Hysteresis loops, (b) Normalized resistance vs. displacement envelopes for the first, second and third cycles.

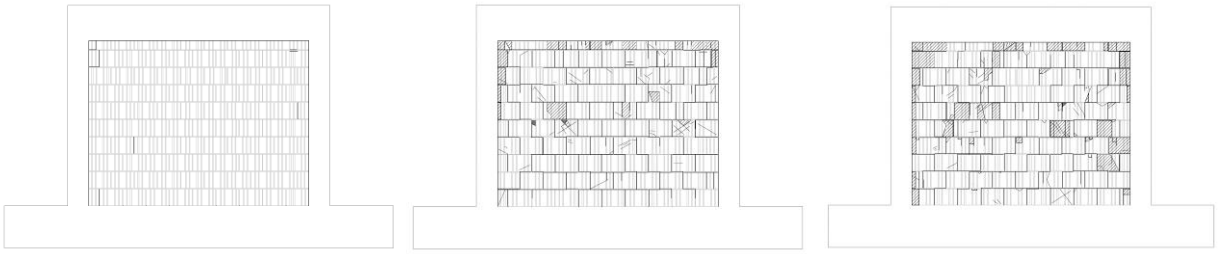

d=0.2% d=2.58%, at maximum resistance d=3.49%, maximum imposed drift

Figure 3. In-plane test of INSYSTEM 2. Crack pattern at various drift values.

Figure 2a shows the hysteresis loops for the tested specimen. Its maximum resistance, equal to 549.0kN,

was mobilized at a drift value equal to 2.58%. The maximum drift applied to the specimen was equal to 3.49%. The hysteresis loop envelopes for the three loading cycles are presented in Figure 2b. One may observe a force-response degradation of the order of 10% during the second loading cycle. Even smaller degradation occurred during the third loading cycle. Finally, a rather stable behavior (characterized by an almost horizontal post-peak curve) is observed after the attainment of the maximum resistance.

Figure 3 shows the damage observed on INSYSTEM 2, for various values of the applied drift. For small values of the applied displacement, only separation of the infill wall from the RC frame was recorded, while no diagonal cracking was observed. It is underlined that cracking of the bricks only occurred for values of the imposed drift higher than 1.00%. One should notice that the damage was concentrated along the bed and head joints. At the maximum achieved drift value (equal to 3.49%), extensive cracking and spalling of bricks in the corner of the infill and along the diagonal was observed.

3. NUMERICAL MODELING

Two different models were used to evaluate the structural function of the reinforced concrete frame and the infill. Firstly, a model of both the frame itself and of the infill was created, in which plane stress conditions were assumed. Analyses on a more detailed model of the standalone masonry infill were also carried out in order to more closely examine the behavior of the infill for different reinforcement schemes. For this model full three-dimensional elasticity was adopted. For both models, embedded reinforcement elements were used for the simulation of the reinforcement bars in both the frame and the infill. The analyses were carried out using the DIANA software package (TNO 2012).

The full frame models include nonlinear interface elements for the simulation of the interaction between the frame and the infill. The interface elements allow for the opening of tensile cracks and the occurrence of shear sliding between the frame and the infill. The horizontal loading was applied as a uniform displacement of the nodes of the top beam and the reaction force was measured at the base of the structure.

For the standalone wall model the interaction of the frame and the infill was simulated by calculating the height of the compression strut according to Mainstone (Mainstone 1971). The loading was applied as a displacement of the nodes within the height of the strut at the upper left corner of the masonry. Similarly, the nodes at the lower right corner of the model within that same height were horizontally restrained, with the total reaction force being measured at those nodes.

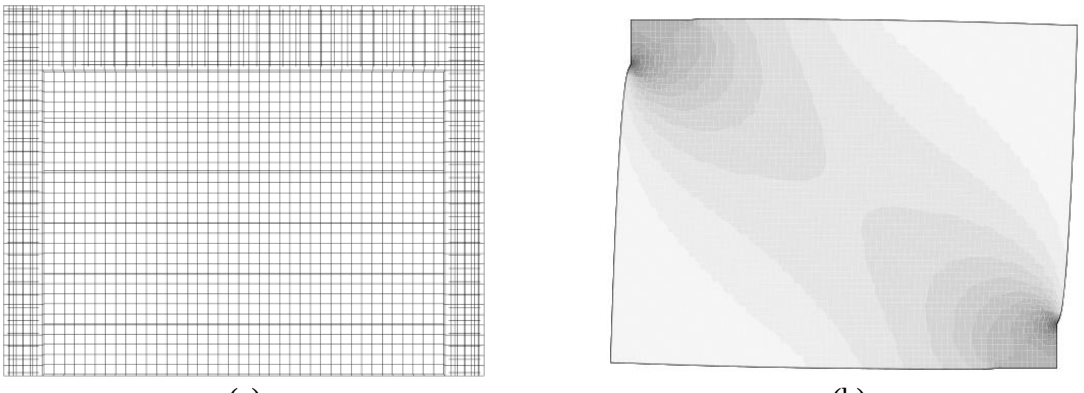

(a) (b)

Figure 4. (a) Finite element models: (a) Full frame with infill and (b) standalone wall (with minimum principal stress distribution indicated).

Both the concrete and the masonry were assigned nonlinear elastic properties. For the simulation of yielding in tension and compression a total strain crack modeling approach was adopted (Selby and Vecchio 1993) using exponential softening in tension and parabolic hardening with ideally plastic post-

peak behavior in compression (Feenstra and Borst 1996). Biaxial behavior is governed by the Hsieh-Ting-Chen failure criterion (Hsieh, Ting, and Chen 1982). The interfaces were prescribed a Mohr-Coulomb failure criterion in shear, combined with a Rankine criterion in tension. Ideally plastic behavior is assumed for the reinforcement bars of the frame and of the infill and no slipping was allowed between the reinforcement and the concrete or masonry.

The material properties assumed for the structural components are as follows:

Table 1. Material properties of structural components.

	E (N/mm^2)	ν (-)	f_c (N/mm^2)	f_t (N/mm^2)	G^I (N/mm)
Concrete	20000	0.20	23	2.3	0.0705
Masonry	500	0.20	1.5	0.15	0.0108
Steel	200000	-	500	500	-
	k_n (N/mm^3)	k_s (N/mm^3)	c (N/mm^2)	$tan(\varphi)$ (-)	f_t (N/mm^2)
Interface	56	20	0.2	0.75	0.2

Four cases were considered for analysis, differentiated according to the layout of the reinforcement bars in the mass of the infill: (a) no reinforcement, (b) horizontal bars only, as in the experiments, (c) vertical bars only and (d) both horizontal and vertical reinforcement. The loading was applied in a monotonic scheme for all the investigated cases and both models.

4. NUMERICAL RESULTS

Full Frame Model

A comparison of the experimental force-displacement envelope curve with the numerically obtained monotonic curve is shown in Figure 5a. Each of the two components of the envelope curve is defined as the maximum reaction force obtained for a given displacement in the positive or negative direction, with both components plotted in the direction of the applied load in the numerical model. Good agreement is found between the two curves, including the post-peak response of the infilled frame. The force-displacement graphs obtained for the full infilled frame models are illustrated in Figure 5b, wherein the curves obtained for all four of the reinforcement layouts are shown. It is mentioned that, the loading of the numerical models was continued to 200mm of in-plane displacement, or more than twice as much as the maximum loading applied in the experiments.

As shown in Figure 5b, the initial global stiffness of the structure is largely unaffected by the presence of reinforcement in either direction compared to the unreinforced configuration. There may be noted, however, a slight increase in the initial stiffness for the simultaneous presence of reinforcement in both directions. More marked, although still modest, is the influence of the reinforcement in the peak force obtained. The horizontal reinforcement afforded a 6.5% increase in the peak force, the vertical reinforcement a 0.5% increase and the combined horizontal and vertical reinforcement provided a 5% increase in the peak force. There may also be noted an improvement of the post-peak ductility of the frame for the same structural configurations, as exhibited by the slope of the curves after the peak. This aspect is most noted in the combined vertical and horizontally reinforced wall for applied deformations greater than 80mm.

Overall, the presence of reinforcement bars in the horizontal direction did not result in any significant improvement of the structural behavior of the infilled frame. However, vertical bars, alone or in combination with horizontal bars, did provide a modest improvement of the attained peak force and ductility.

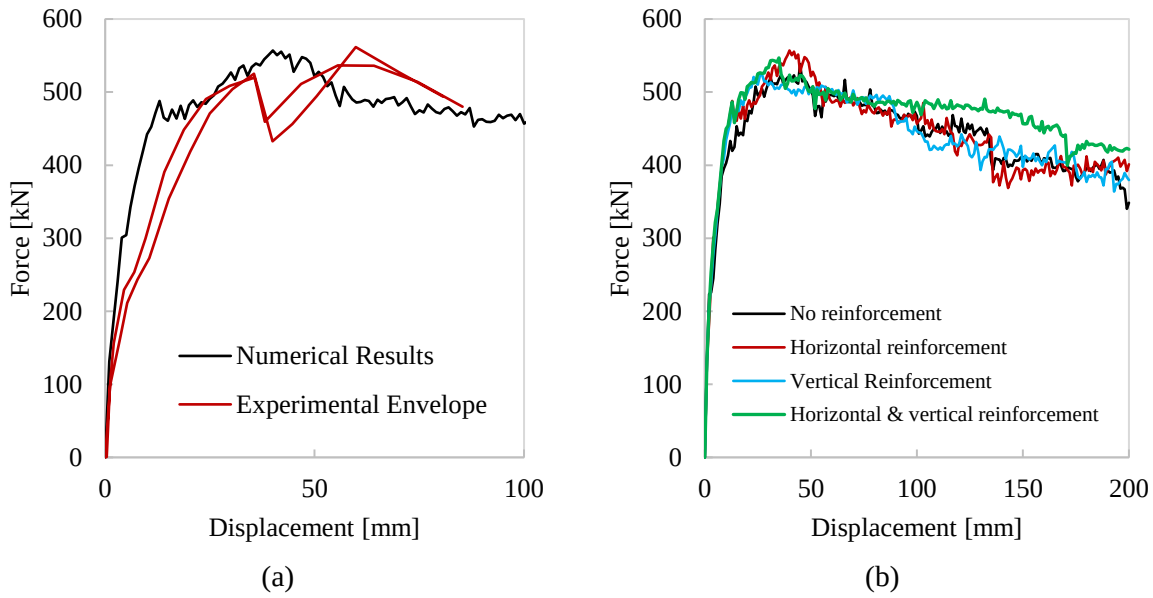

Figure 5. (a) Comparison of the force-displacement experimental envelope with the full frame numerical model with horizontally reinforced infill. (b) Comparison of full frame model numerical results for different layouts of infill reinforcement.

The numerically obtained damage patterns on the infills, in terms of crack width, are shown in Figures 6 and 7, with the former indicating the crack widths at 5mm of applied deformation and the latter at 80mm. The loading direction was from left to right.

For all the cases there was a small degree of cracking registered at the reinforced concrete columns around the contact area with the infill, where additionally yielding of the stirrups was registered. For an applied deformation of 5mm, the general orientation of the major cracks was similar. However, in the presence of reinforcement these cracks were more diffuse and generally of a noticeably smaller width, particularly in the case of the wall reinforced both in the vertical and horizontal direction. The cracks generally appear at the location of the reinforcement bars, meaning that the units may remain undamaged for small values of the applied displacement loads, while maintaining the overall diagonal direction. The maximum values of the crack width were 1.75mm for the unreinforced wall, 1.91mm for the horizontally reinforced wall, 0.89mm for the vertically reinforced wall and 0.82mm for the wall reinforced vertically and horizontally.

For an applied displacement of 80mm several differences are noted in the layout of the cracks between the different wall structures. The initial cracks registered at the unreinforced wall continue to develop, forming two major cracks initiating at the area of contact between the wall and the frame. These cracks have a maximum opening of roughly 39.3mm. Similar cracks are formed in the reinforced walls, with their extent and their maximum opening width being smaller: 36.4mm for the horizontally reinforced walls, 37.7mm for the vertically reinforced walls and 33.5mm for the walls reinforced vertically and horizontally. There was formed, however, in all the reinforced wall cases a large shear crack at the mid height of the wall. A large portion of the overall deformation of the wall is accounted for at this sliding failure, located at the position of a reinforcement bar.

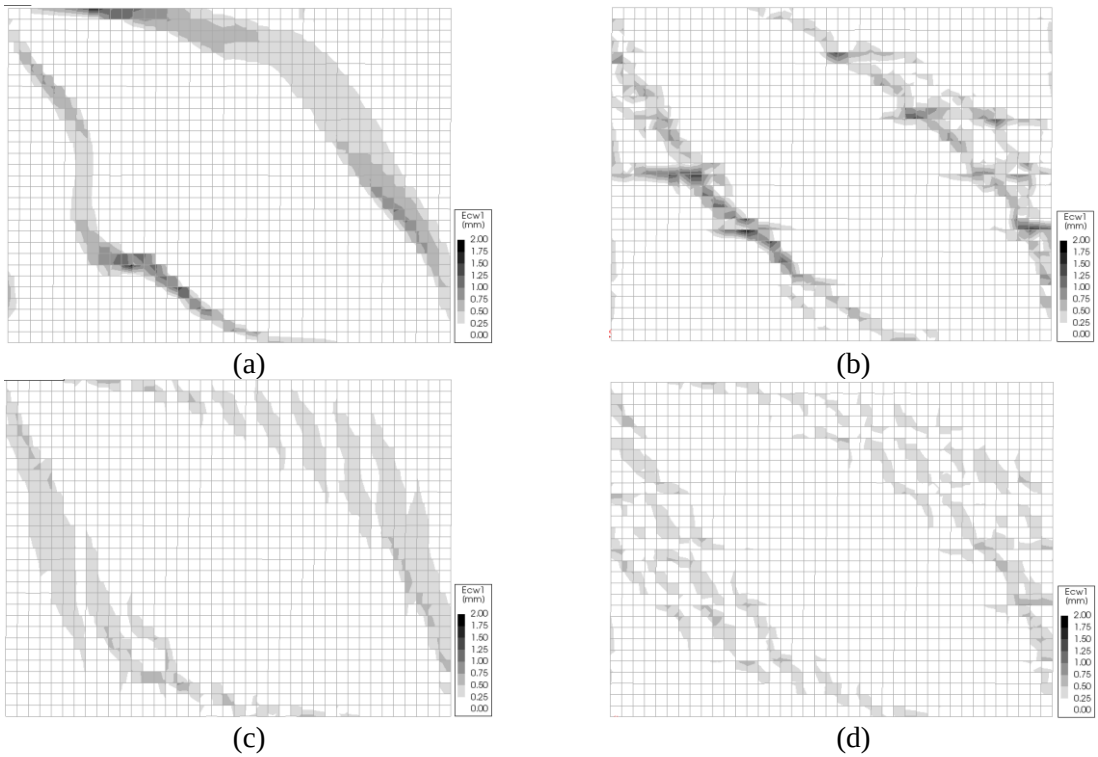

Figure 6. Masonry damage patterns in full frame models at 5mm applied displacement: (a) no reinforcement, (b) horizontal bars only, (c) vertical bars only and (d) horizontal and vertical reinforcement.

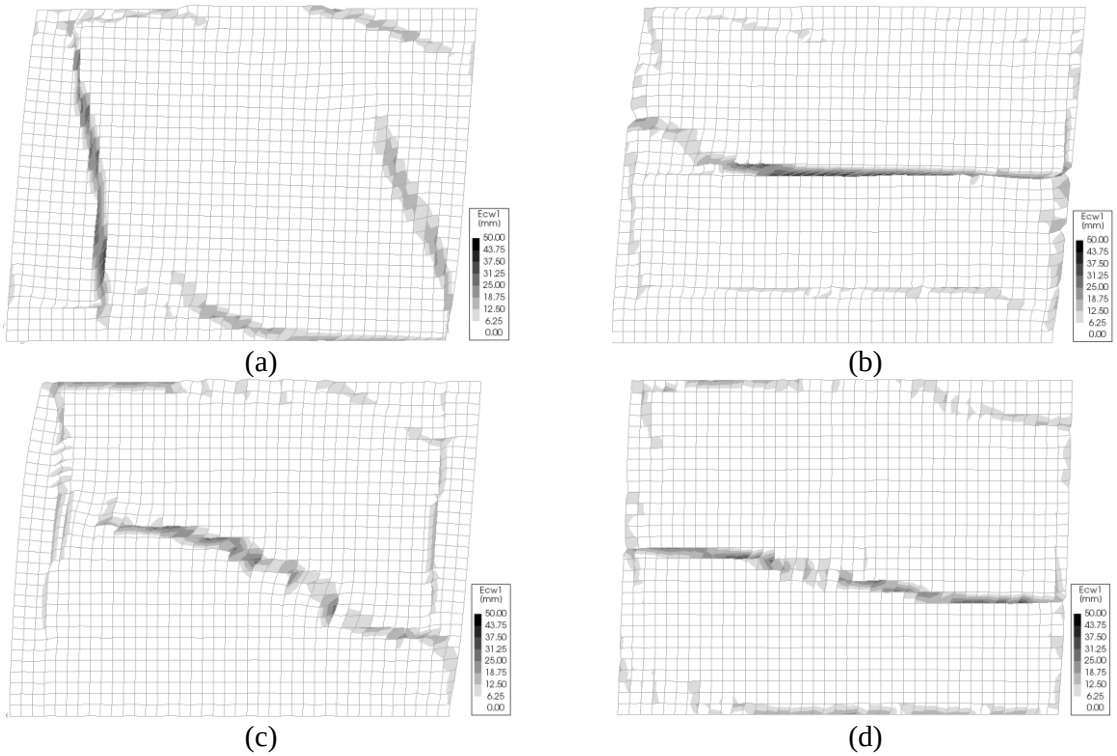

Figure 7. Masonry damage patterns in full frame models at 80mm applied displacement: (a) no reinforcement, (b) horizontal bars only, (c) vertical bars only and (d) horizontal and vertical reinforcement.

Standalone Infill Model

The force-displacement diagrams obtained for the stand-alone wall models are shown in Figure 8. One may observe that the analyses confirm the results of the analyses carried out on the full frame plane stress model. For all the examined cases, the initial structural stiffness was unaffected by the reinforcement pattern. Slight differences were registered in the peak force obtained. While the unreinforced, vertically reinforced and horizontally reinforced walls attained a peak force or about 180kN, the vertically and horizontally reinforced wall attained a peak force of only 170kN, a 5.5% relative reduction.

It is important to note that while the peak resistance of the stand-alone walls was roughly 36% that of the infilled frame, the displacement for which the peak force is attained is much lower than that of the complete structural system: the peak force was reached at roughly 9mm displacement for the walls, while the infilled frames reached their peak capacity at roughly 37mm.

The main difference in the response of the stand-alone wall models is noted in the obtained post-peak behavior. The unreinforced wall exhibited, as expected, a very brittle post peak behavior, immediately dropping to 50% of its capacity and exhibiting a residual strength of roughly 40kN. The vertically reinforced wall dropped to 65% of its capacity and exhibiting a residual strength of 70kN. The horizontally reinforced wall exhibited a secondary peak force at 66% of the initial peak and a residual force equal to that of the unreinforced wall. The both vertically and horizontally reinforced wall were the only models that exhibited any true post peak ductility, exhibiting a force plateau from 8mm to 13mm displacement.

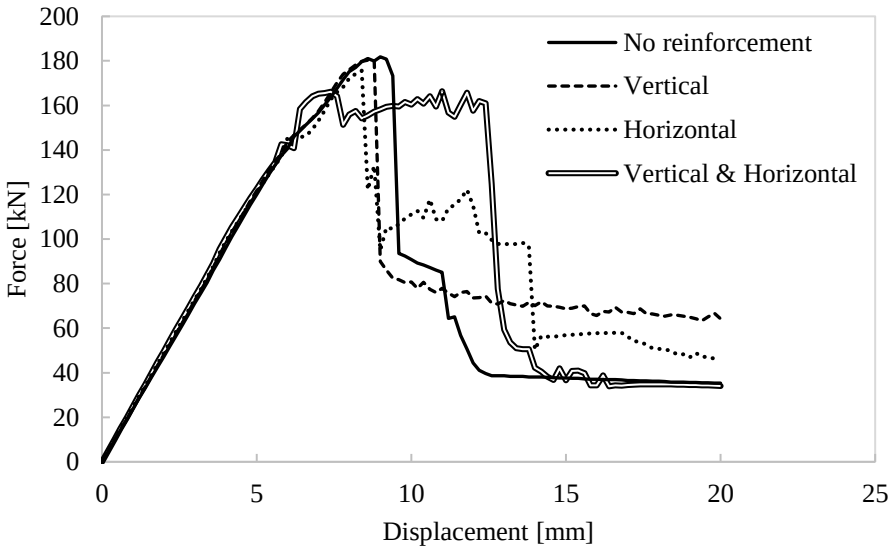

Figure 8. Force-displacement graphs for standalone wall models with different reinforcement schemes for the infill.

The damage patterns obtained for the stand-alone wall models are shown, in terms of crack strains, in Figure 9 for an applied displacement of 9mm, roughly corresponding to the point of attainment of the peak force. The localized cracks noted at the loaded corners of the infill were also registered in the stand-alone wall models. Cracking damage was largely localized at those locations. The horizontally reinforced wall was characterized by a more diffuse damage pattern, accented by the presence of the reinforcement bars. The vertically reinforced wall was characterized by a similar behavior, but rather less distributed cracking pattern. Finally, the vertically and horizontally reinforced wall presented a main diagonal crack, expanding at its intersections with the reinforcement bars at the central area of the wall. The maximum crack width for each wall at this particular deformation load level are: 5.5mm for the unreinforced wall, 4.1mm for the horizontally reinforced wall, 4.9mm for the vertically reinforced wall and 3.7mm for the wall reinforced vertically and horizontally. This suggests that, mainly, the presence

of the horizontal reinforcement reduces significantly the maximum crack width.

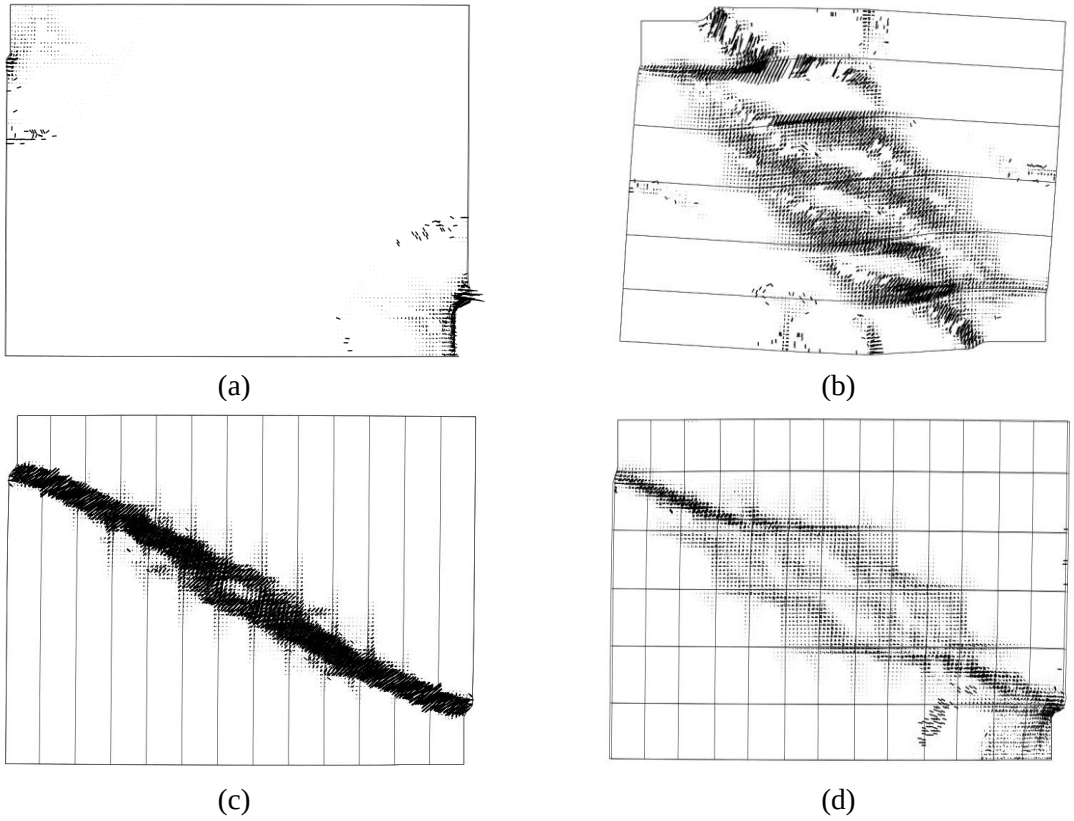

Figure 9. Damage patterns in standalone wall models: (a) no reinforcement, (b) horizontal bars only, (c) vertical bars only and (d) horizontal and vertical reinforcement.

The main failure mode obtained for the standalone walls was that of compressive yielding at the location of the loaded surfaces. As shown in the distribution of the minimum principal stresses in Figure 4b, the highest compressive stresses are concentrated near the contact areas with the frame. This results in the localized failure of the infill. In the absence of reinforcement, no continuous cracks were registered in the infill.

In a final illustration of the structural behavior of the stand-alone walls, the obtained force-displacement graphs were added to the force-displacement graph of a bare frame of the same configuration and the resulting curves are compared to each other and with the experimental envelope (Figure 10). The experimental envelope is defined as the force envelope obtained between the loading cycles in the two in-plane directions during experimental testing. Overall, all the composite curves are close to the experimental envelope. For all the cases a marked reduction of the overall stiffness is noted following the failure of the walls, with the both horizontally and vertically reinforced wall maintaining its stiffness for a slightly higher displacement. It is interesting to note that at the point of failure of the masonry, the infill is bearing roughly 50% of the total horizontal load applied on the full structure.

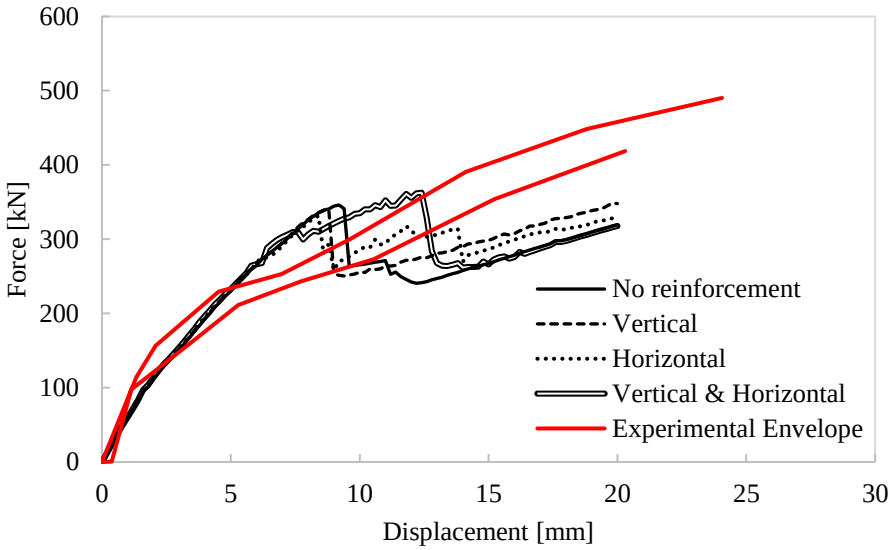

Figure 10. Comparison of stand-alone wall numerical results, added to bare frame numerical results, with experimental results.

5. CONCLUSIONS

The influence of embedded steel reinforcement in masonry infills of reinforced concrete frames was investigated in this paper using numerical modeling. For this purpose, two models were developed: a full frame plane stress model, in which all the RC frame, the masonry infill and the interfaces between the frame and the wall were modeled, and a stand-alone 3D model, in which only the masonry enclosure was simulated. For each model, the reinforcement of the masonry infill was employed in different layouts within the body of the masonry. The results of these analyses show that, while the effect of the reinforcement on the peak force and the structural stiffness of the infill is rather limited, the increase in the post-peak behavior and the observed damage pattern is more marked. The presence of vertical reinforcement enhances the post-peak response of the infill, whereas the horizontal reinforcement mostly attains the diffusion of damage on the body of the infill and reduces the maximum crack width. The concentration of damage in the position of the embedded reinforcement is indicative of the potential for minimizing irreversible damage to the infill, namely damage to the masonry units. Additionally, this potential is further increased by the apparent, though only modest, increase of the ductility of the reinforced infill. In the case of low seismicity events the economic benefit of reduction of damage to the infill can be substantial.

6. AKNOWLEDGMENTS

This research has received funding from the Europe-an Union's Seventh Framework Programme for re-search, technological development and demonstration under grant agreement No 606229, http://www.insysme.eu/.

7. REFERENCES

Calvi, Gian Michele and D. Bolognini. 2001. "Seismic Response of Reinforced Concrete Frames Infilled with Weakly Reinforced Masonry Panels." *Journal of Earthquake Engineering* 5(2):153–85.

CEN. 2005. *EN 1998-3 - Eurocode 8: Design of Structures for Earthquake Resistance - Part 3: Assessment and Retrofitting of Buildings*.

Ezzatfar, Pourang et al. 2014. "Application of Mesh Reinforced Mortar for Performance Enhancement of Hollow Clay Tile Infill Walls." Pp. 171–86 in *Seismic Evaluation and Rehabilitation of Structures*, edited by A. Ilki and M. N. Fardis. Cham: Springer International Publishing.

Facconi, L., A. Conforti, F. Minelli, and G. A. Plizzari. 2012. “Shear Strength Improvement of Unreinforced Masonry Walls by Means of High Performance Steel Fibre Rein¬forced Mortar.” in *Proceedings of the 8th RILEM International Symposium (BEFIB 2012), 19-21 September, Guimaraes, Portugal*.

Feenstra, P. H. and René De Borst. 1996. “A Composite Plasticity Model for Concrete.” *International Journal of Solids and Structures* 33(5):707–30.

Ghobarah, A. and K. Mandooh Galal. 2004. “Out-of-Plane Strengthening of Unreinforced Masonry Walls with Openings.” *Journal of Composites for Construction* 8(4):298–305.

Hsieh, S. S., E. C. Ting, and W. F. Chen. 1982. “A Plastic-Fracture Model for Concrete.” *International Journal of Solids and Structures* 18(3):181–97.

Leite, J. and Paulo Lourenço. 2012. “Solutions for Infilled Masonry Buildings: Shaking Table Tests.” in *Proceedings of the 15th International Brick and Block Masonry Conference, 3-6 June, Florianópolis, Brazil*.

Mainstone, R. J. 1971. “On the Stiffnesses and Strengths of Infilled Frames.” in *Proceedings of the Institution of Civil Engineers, Vol. 4*.

Masia, Mark J., G. Simundic, and Adrian W. Page. 2016. “Flexural Strength of Stack Bonded Masonry in One Way Horizontal Bending: Influence of Bed Joint Reinforcement.” in *Proceedings of the 16th International Brick and Block Masonry Conference “Masonry in a World of Challenges”, 26-30 June, Padova, Italy*.

Penna, Andrea, Gian Michele Calvi, and D. Bolognini. 2007. “Design of Masonry Structures with Bed Joint Reinforcement.” Pp. 21–40 in *Proceedings of the Portuguese Seminar “Paredes de Alvenaria: Inovação e Possibilidades Actuais”, University of Minho and LNEC, Lisbon*.

Da Porto, F., Giovanni Guidi, Massimo Dalla Benetta, and N. Verlato. 2013. “Combined in-Plane/out-of-Plane Experimental Behaviour of Reinforced and Strengthened Infill Masonry Walls.” in *Proceedings of the 12th Canadian Masonry Symposium, 2-5 June, Vancouver, British Columbia*.

Da Porto, F., Giovanni Guidi, N. Verlato, and Claudio Modena. 2015. “Effectiveness of Plasters and Textile Reinforced Mortars for Strengthening Clay Masonry Infill Walls Subjected to Combined in-Plane/out-of-Plane Actions.” *Mauerwerk* 19(5):334–54.

Selby, R. G. and F. J. Vecchio. 1993. *Three-Dimensional Constitutive Relations for Reinforced Concrete*. University of Toronto, Department of Civil Engineering.

TNO. 2012. *DIANA User’s Manual*. Delft: TNO DIANA BV.

Vermeltfoort, Arduïnus. 2016. “Bed Joint Reinforcement and the Load Bearing Capacity of Masonry Beams.” in *Proceedings of the 16th International Brick and Block Masonry Conference “Masonry in a World of Challenges”, 26-30 June, Padova, Italy*.

Vintzileou, Elizabeth and V. Palieraki. 2007. “Perimeter Infill Walls: The Use of Bed Joint Reinforcement or RC Tie-Beams.” *Journal Masonry International* 20(3):117–28.

Vintzileou, Elizabeth, V. Palieraki, Chrissy-Elpida Adami, and V. Nikolopoulou. 2017. “In-Plane and out-of-Plane Response of a Reinforced Masonry Infill Made by an Innovative New Brick Unit.” in *Proc. 16th World Conference on Earthquake Engineering, Santiago, Chile*.